Effect of mesoporosity against the deactivation of MFI zeolite catalyst during the methanol-to-hydrocarbon conversion process

Jeongnam Kim [a,b], Minkee Choi [a], Ryong Ryoo [a,b,c,*]

[a] Center for Functional Nanomaterials and Department of Chemistry, KAIST, Daejeon 305-701, Republic of Korea
[b] Graduate School of Nanoscience and Technology (WCU), KAIST, Daejeon 305-701, Republic of Korea
[c] KAIST Institute for the NanoCentury, Daejeon 305-701, Republic of Korea

ARTICLE INFO

ABSTRACT

The effects of mesoporosity on catalyst longevity of methanol-to-hydrocarbon (MTH) reactions have been investigated using a number of MFI zeolites with different degrees of mesoporosity, which were obtained via the post-synthetic desilication, dry-gel conversion in nanocarbon templates, and hydrothermal synthesis with the addition of organosilane surfactants. The MTH catalytic lifetime could be increased by more than three times due to the generation of mesopores. The cause for catalyst longevity was investigated by probing the location of coke that formed during the reaction using argon adsorption measurements. The result showed that the coke formed mainly on mesopore walls in the case of mesoporous zeolite. On the other hand, the coke was more heavily deposited inside micropores in the case of solely microporous zeolites. The short diffusion path lengths and hence facile diffusion of coke precursors were most likely the cause of the improvement in the catalytic lifetime.

Crown Copyright © 2009 Published by Elsevier Inc. All rights reserved.

1. Introduction

Searching for future energy sources as alternatives to crude oil is one of the most important issues among current scientific topics. Among several alternatives, the conversion of synthesis gas (syngas in short, a mixture of CO and H_2) into hydrocarbons has long been of great interest in the petrochemical industry as a potential means of providing fuels and raw materials for petrochemical products in the future when crude oil becomes more expensive to obtain [1,2]. Syngas is produced via a reforming or gasification process of coal, natural gas, and biomass, which are much more abundant than crude oil. The Fischer–Tropsch (FT) process is a well-known process of converting syngas to hydrocarbons. It generates diesel fuels and waxes using Co- or Fe-based catalysts [3]. SASOL has operated FT-based plants for several decades, and is currently planning to increase their operational capacity to 34,000 barrels per day [4]. As an alternative to the FT process, methanol can be mass-produced from syngas. Methanol can then be converted to hydrocarbons such as light olefins, high-octane gasoline, and other value-added chemicals over acidic zeolite or zeolite-type catalysts [5–8]. This process is known as the methanol-to-hydrocarbon (MTH) conversion process.

The MTH process has a remarkable advantage in terms of product selectivity stemming from its use of zeolite or zeolite-type catalysts, as compared to the FT process [5]. Zeolites are crystalline aluminosilicate minerals possessing strong acid sites within the regular arrangement of its uniform micropores [9]. The uniform microporosity imparts product shape selectivity in the MTH reaction to zeolites. For example, HZSM-5 zeolite having an MFI pore topology with a crystallographic pore diameter of 0.56×0.53 nm is suitable for the production of gasoline-range hydrocarbons. Moreover, light olefins such as ethene and propene can be selectively obtained using zeolites with smaller pore apertures ($\sim$0.4 nm). Generally, such MTH reactions are referred to as methanol-to-gasoline (MTG) and methanol-to-olefin (MTO) reactions, depending on the target products.

Since its discovery by Mobil during the first world oil crisis [10], great efforts have been devoted toward practical applications of the MTH reaction. There have been numerous investigations related to the MTH reaction, including an in-depth study of the reaction mechanisms [5,7,11–14], process studies [8], and studies that seek to control product selectivity via catalyst modifications [5,15]. The first commercial MTG plant was constructed in Motunui [16]. In 1986, the Motunui plant began producing 14,450 barrels per day of gasoline using ZSM-5 catalysts. However, after operating for 10 years, the plant for gasoline production was closed after a

significant drop in crude oil prices. Recently, the MTO process using SAPO-34 catalysts was demonstrated as a demo plant [17], and a methanol-to-propene process, developed by Lurgi, is ready for commercialization [13].

During MTH operations, unfortunately, zeolite catalyst is rapidly deactivated by the deposition of carbonaceous residues (generally referred to as coke) which block the reactants from accessing the active sites [6]. Hence, the MTH process requires frequent regeneration of the catalyst. The formation of coke on the catalyst is an important cost-bearing factor not only in the MTH process but also in many other petrochemical processes using zeolite catalysts, including hydrocarbon refining and fine-chemical syntheses [18,19]. It is, therefore, very important to investigate the structural factors of zeolite that can affect coke deposition and catalyst deactivation.

Mesoporous zeolite is a material that can be characterized by secondary mesoporosity in addition to structural microporosity. Recently, mesoporous zeolites have been obtained in a number of routes [20–22] including post-synthetic steaming, alkali treatment [23], and synthesis in the presence of mesopore-generating agents such as carbon nanoparticles [24], silylated organic polymers [25] and organosilane surfactants [26]. The zeolites with such hierarchically mesoporous/microporous structures (hereafter, mesoporous zeolites or hierarchical zeolites) exhibit high catalytic activity in reactions involving bulky molecules that are too large to enter the micropores due to the catalytic activity of the mesopore walls [27,28]. These hierarchical zeolites show a significant change in product selectivity in reactions that are catalyzed by acid sites inside the micropores. This change can be attributed to enhanced diffusion to and/or from the reaction sites in micropores through the mesopores [29,30]. A more remarkable phenomenon, in relation to the hierarchically porous structure, is the significantly enhanced catalytic lifetime in some catalytic reactions that are believed to have occurred inside the zeolite micropores. As reported by Srivastava et al., hierarchical MFI zeolites are deactivated at a much slower pace compared to conventional MFI zeolite (i.e., ZSM-5) in various reactions [31]. Catalytic lifetimes were also reported to increase in MTH reactions [32,33] although the change was not as obvious compared to the reactions reported by Srivastava et al. The catalytic longevity was attributed to facile molecular diffusion through the mesopores. However, how the mesopore generation or fast diffusion could lead to catalytic longevity remained unanswered.

The present study was undertaken to understand why the catalytic lifetime in MTH reactions is improved via the generation of secondary mesoporosity within MFI zeolite. To understand this, hierarchical MFI zeolites were synthesized by a synthesis route using organosilane surfactants as the mesopore generator [26]. The amounts of the organosilane surfactants were varied for systematic control of the mesoporosity in the zeolites. Hierarchical MFI zeolites were also synthesized using other methods, in this case desilication and carbon-templating. The catalytic lifetimes in the MTH reactions of these zeolites were monitored in relation to the formation and location of coke in the micropores or mesopores. Argon adsorption was used to understand where the coke is generated during this process.

2. Experimental

2.1. Catalyst samples

2.1.1. Zeolite preparation

Two zeolite samples with an MFI structure were purchased in the NH_4^+ ion-exchanged form from Zeolyst (CBV 3024E with Si/Al = 12, and CBV 8014 with Si/Al = 40). The samples were calcined in air under static conditions at 823 K prior to use as a catalyst for MTH reactions. These samples are designated here as ZST-12 and ZST-40, according to the Si/Al ratios. Two additional samples of MFI zeolite were synthesized using 3-[(trimethoxysilyl)propyl]hexadecyldimethylammonium chloride (TPHAC) as a mesopore-directing organosilane surfactant. The zeolite synthesis procedure was identical to that reported previously, apart from the substitution of sodium aluminate by aluminum sulfate [27]. The molar composition of the synthesis gel was 40 Na_2O: 100 SiO_2: 2.5 Al_2O_3: 10 tetrapropylammonium bromide (TPABr): 26 H_2SO_4: n TPHAC: 9000 H_2O, where n was either 2 or 5. The samples were subsequently calcined in air at 823 K. The synthesized samples had Si/Al ratios in the range of 13–14 (Table 1). The organosilane-directed zeolites are denoted as OSD-n, where OSD denotes 'organosilane-directed' and n refers to the number of TPHAC moles.

TPHAC was synthesized in our laboratory by reacting 3-(chloropropyl)trimethoxysilane (CPTMS, 97%, Sigma–Aldrich) with N,N-dimethylhexadecylamine (DMHDA, 95%, Sigma–Aldrich) in anhydrous methanol (99.8%, Sigma–Aldrich). In a typical experiment, 43.8 g (0.22 mol) of CPTMS and 54.0 g (0.20 mol) of DMHDA were dissolved in 128 g (4.0 mol) of methanol. The resultant solution was heated at 383 K while stirring for 36 h in a Teflon-lined stainless steel autoclave. After cooling to room temperature, the product was concentrated to a 64 wt% methanol solution in a rotary evaporator and used without further purification steps. TPHAC may be substituted by 3-[(trimethoxysilyl)propyl]octadecyl-dimethylammonium chloride, which is available from Sigma–Aldrich or Acros.

The details of the OSD-5 synthesis process can be briefly described as follows: 1.5 g of TPHAC (64 wt% in methanol) was dissolved under magnetic stirring in a solution consisting of 2.7 g of TPABr, 1.1 g of NaOH, and 50 g of water at 333 K. 44.7 g of an aqueous solution of sodium silicate (Si/Na = 1.75, 15 wt% SiO_2) was added to the TPHAC solution under vigorous stirring. The resultant mixture was aged at 333 K for 12 h while stirring. A solution consisting of 1.5 g of aluminum sulfate octadecahydrate (98%, Sigma–Aldrich), 1.8 g of H_2SO_4 (99%), and 75 g of water was added dropwise into the resulting mixture under vigorous stirring. The final synthesis mixture was aged further at room temperature for 3 h, and this was followed by heating while stirring at 415 K for 4 d in a Teflon-coated stainless steel autoclave. After cooling to room temperature, the zeolite product was filtered and washed thoroughly with deionized water. The product was dried in an oven at 403 K and subsequently calcined in air at 823 K for 4 h.

Two additional types of MFI zeolite possessing mesopores were obtained via a post-synthetic treatment using NaOH [23] and a hydrothermal synthesis procedure using carbon black as a template [24], respectively. The zeolite samples are designated here as BTZ-13 and CTZ-16, respectively. BTZ represents 'base-treated zeolite', CTZ 'carbon-templated zeolite', and the numbers are the Si/Al ratios. The preparation of BTZ-13 proceeded as follows: A ZSM-5 zeolite with Si/Al = 25 was synthesized by the same procedure used for OSD-5, except that TPHAC was used in this case. This zeolite was calcined at 823 K and then agitated in a 0.2 M NaOH solution at 333 K for 30 min. The CTZ-16 sample was obtained through the same dry-gel synthesis procedure developed by Jacobsen et al. [24], except that a carbon black sample (CABOT RAVEN1200, average particle size of 20 nm) was used at a gel composition of 40 Na_2O: 100 SiO_2: 2.5 Al_2O_3: 10 TPABr: 26 H_2SO_4.

All the zeolite samples synthesized in the present work were calcined at 823 K, ion exchanged three times with 1 M of NH_4NO_3 solution into the NH_4^+ form, and calcined again at 823 K for conversion to the H^+ form.

2.1.2. Dealumination

The OSD-5 zeolite in the H^+ form was dealuminated by two procedures using L-tartaric acid (Sigma–Aldrich) and ammonium

Table 1
Chemical composition and textural properties of MTH catalysts used in the present study.

Catalyst[a]	Si/Al	S_{BET} ($m^2 g^{-1}$)	D_{BJH} (nm)	V_{micro} ($cm^3 g^{-1}$)	V_{meso} ($cm^3 g^{-1}$)	S_{ext} ($m^2 g^{-1}$)
ZST-12	11.8	388	–	0.14	0.07	46.8
ZST-40	40.1	420	–	0.15	0.08	97.0
OSD-2	13.7	444	4.3	0.12	0.31	262
OSD-5	13.0	524	3.9	0.11	0.32	392
BTZ-13	12.8	402	–	0.12	0.19	145
CTZ-16	16.0	342	>30	0.12	0.23	78.0
TA-OSD-5	25.3	514	4.1	0.11	0.35	373
FS-OSD-5	20.7	510	3.9	0.11	0.29	339

[a] The numbers indicate Si/Al ratio obtained by ICP–AES analysis; S_{BET} is the apparent BET surface area; D_{BJH} is the mesopore diameter calculated using the BJH method; V_{micro} is the micropore volume calculated from Saito–Foley method; V_{meso} is the mesopore volume; and S_{ext} is the external surface area evaluated from the *t*-plot method.

hexafluorosilicate (Sigma–Aldrich), respectively. For the tartaric acid treatment [27], 1 g of sample was added to 20 mL of 1 M of L-tartaric acid solution. The slurry was stirred at 333 K for 4 h. For dealumination with fluorosilicate (FS) [34], 1 g of OSD-5 was treated with 10 mL of 0.1 M of FS solution at room temperature for 30 min. After dealumination, the zeolites were filtered, washed with deionized water, and dried at 373 K. The samples were denoted as TA-OSD-5 and FS-OSD-5. Here, TA refers to 'tartaric acid' and FS stands for 'fluorosilicate'.

2.2. Characterization methods

Si/Al ratios were determined by inductively coupled plasma-atomic emission spectroscopy (ICP-AES) using an OPTIMA 4300 DV instrument (Perkin Elmer). X-ray diffraction patterns (XRD) were determined by a Rigaku Multiflex diffractometer equipped with a Cu K_α radiation (40 kV, 40 mA). Argon adsorption–desorption isotherms were measured volumetrically at the temperature of liquid Ar (87 K) using a Micromeritics ASAP 2020 instrument. The samples were degassed for 4 h at 623 K under vacuum prior to the adsorption measurements. The Brunauer–Emmett–Teller (BET) equation was used to calculate the apparent surface area from the adsorption data obtained in the pressure range $P/P_0 = 0.05–0.2$. The pore size distribution was calculated by the Barrett–Joyner–Halenda (BJH) method using the adsorption branch. The micropore volume was evaluated using the Saito–Foley method [35]. Scanning electron micrographs (SEM) were obtained with a Hitachi S-4800 microscope operating at 2 kV without a metal coating. Transmission electron microscopy (TEM) images were taken from the thin edges of particles supported on a porous carbon grid using a JEOL JEM-2100F device operating at 200 kV.

Temperature-programmed desorption (TPD) of NH_3 was measured in a He flow using an instrument (BELCAT-M, BEL Japan) equipped with a thermal conductivity detector (TCD). Before the measurement, 50 mg of zeolite was degassed in a He stream (20 mL min^{-1}) at 773 K for 1 h. After cooling to 373 K, the sample was put in a mixed gas flow of 10 mol% NH_3 and 90% He (20 mL min^{-1}) for the sufficient adsorption of the NH_3. Subsequently, the sample was exposed to flowing He for 3 h to remove weakly adsorbed NH_3. Finally, a TPD profile was obtained while the sample was heated from 373 to 923 K at a ramping rate of 10 K min^{-1} under flowing He (20 mL min^{-1}). The TPD profile thus obtained was deconvoluted with the assumption of Gaussian distributions.

The number of external acid sites in MFI zeolites was determined by the chemisorption of 2,6-di-*tert*-butylpyridine (DTBPy) using a high-accuracy magnetic suspension balance (Rubotherm, sensitivity = 0.01 mg). Details of this experimental method are described in a previous work by the authors [27]. The experimental procedure is briefly described here. Prior to the adsorption of DTBPy, the zeolite sample was degassed overnight under a vacuum

at 623 K. After being cooled to room temperature, the sample was exposed to DTBPy until saturation and was subsequently evacuated at 393 K for 4 h to remove any weakly adsorbed DTBPy molecules. The weight changes before and after adsorption were recorded and then converted into the number of external acid sites with the assumption of one DTBPy molecule per acid site.

2.3. Reaction measurement

An MTH reaction was performed at 673 K in a fixed bed Pyrex reactor (inside diameter = 13 mm) using 0.1 g of zeolite as a catalyst. The reaction temperature was measured by a K-type thermocouple inserted in the reactor through a thermocouple well. Before the reaction, the catalyst was activated at 823 K for 2 h under an air flow (30 mL min^{-1}). The catalyst bed was put in contact with a high-purity N_2 flow (50 mL min^{-1}) which was saturated with methanol (99.6%) at 298 K through a bubble saturator. The bubbler temperature was maintained by a constant temperature bath. The methanol feeding rate was estimated from the gas flow rate and the saturation vapor pressure of the methanol vapor. A weight hourly space velocity (WHSV) was 7.5 g g^{-1} h^{-1} under this condition. The reactor effluent was analyzed by two online gas chromatographs (GC, Younglin, Acme-6000) equipped with a flame ionization detector [36]. One GC was equipped with a capillary column (HP-Plot-Q, J&W) for accurate measurement of the total MTH conversion. The other GC used another type of capillary column (GasPro, J&W) for the relative determination of $C_1–C_{12}$ hydrocarbons. By considering oxygenates (methanol and dimethylether) as unconverted species, the conversion was calculated on the basis of a GC analysis. To avoid the condensation of heavy compounds, the connecting lines between reactor and GC were heated to temperatures in excess of 373 K.

2.4. Coke analysis

An MTH reaction was carried out with a 0.1 g of catalyst sample at 673 K until a targeted conversion level or time-on-stream level was reached. Subsequently, the reactor was purged with a high-purity N_2 gas flow (50 mL min^{-1}) for 3 h at 673 K to remove organic volatiles. A portion of the sample was taken for thermogravimetric analysis (TGA). The temperature was increased to 873 K under flowing air (60 mL min^{-1}) at a constant ramping rate of 10 K min^{-1} (TGA Q500, Thermal Analysis Instruments Inc.). The sample weight loss between 573 and 873 K was taken as the total coke content. Another portion of the nitrogen-purged sample was taken for Ar adsorption measurements. Adsorption was measured at 87 K using the procedure described above. The micropore volume was determined from the adsorption isotherm at low pressure, according to the Saito–Foley method. The amount of internal coke in the zeolite micropores was determined from the decrease in the micropore volume, as compared with a pristine sample. This

analysis is based on the assumption that the remaining micropore volume is fully accessible to Ar molecules through the three dimensionally interconnected zeolite channels [37,38]. The internal coke content was calculated with the assumption that the coke density was 1.22 g cm^{-3}. This density is based on a C/H ratio of 1.25, similar to that of coal [37,38]. The amount of external coke (i.e., coke deposition on the external surface) was calculated by subtracting the internal coke content from the total coke content.

3. Results

3.1. Porosity and acidity

All zeolite samples obtained in this work exhibited powder XRD patterns that were characteristic of a fully crystalline MFI structure, as represented in Fig. 1. The XRD patterns showed no background increase in the 2θ region of 15–25°, which can be attributed to the presence of non-crystalline impurities. The XRD line widths for OSD-2 and OSD-5 in Fig. 1 were broader than those for ZST-12 zeolite. This broadening was due to a decrease in the crystallite thickness in the case of the OSD samples rather than to poor crystallinity [26].

Fig. 2 shows representative SEM and TEM images obtained for ZST-12, OSD-2, and OSD-5. As shown by the electron micrographs, ZST-12 was composed through the aggregation of primary crystals with a wide distribution of particle diameters in a range of 50–200 nm. OSD-2 exhibited crystal thicknesses that ranged from 20 to 40 nm in the outer part of the agglomerate. OSD-5 exhibited 10–20 nm. However, such measurements at the outer part could overestimate the crystal thickness, whereas the crystal ripening
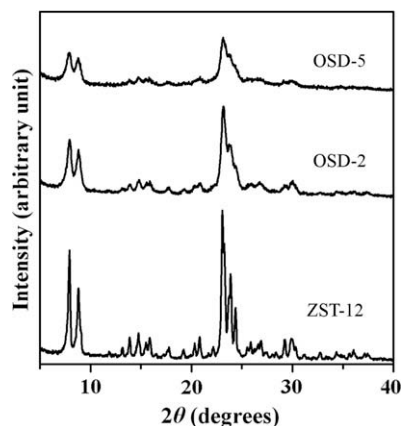

Fig. 1. Powder XRD patterns of ZST-12 (i.e., commercial HZSM-5, Si/Al = 12) and OSD-*n* zeolites prepared by adding different amounts of TPHAC as mesopore generators. '*n*' indicates the number of TPHAC moles in the ZSM-5 gel composition: 40Na$_2$O/100SiO$_2$/2.5Al$_2$O$_3$/10TPABr/26H$_2$SO$_4$/9000H$_2$O/*n* TPHAC.

process can lead to an increase in the crystal thickness apparently in the outside zone of OSD particles [26]. A close examination of the TEM images revealed that the OSD samples possessed disordered mesoporous structures with nano-crystalline MFI frameworks [26]. The individual crystallite thickness decreased as the amount of TPHAC increased in the synthesis composition, which is consistent with the XRD broadening shown in Fig. 1.

The OSD-5 sample had a much higher BET area and a larger mesopore volume (524 m^2 g^{-1} and 0.32 cm^3 g^{-1}, respectively)
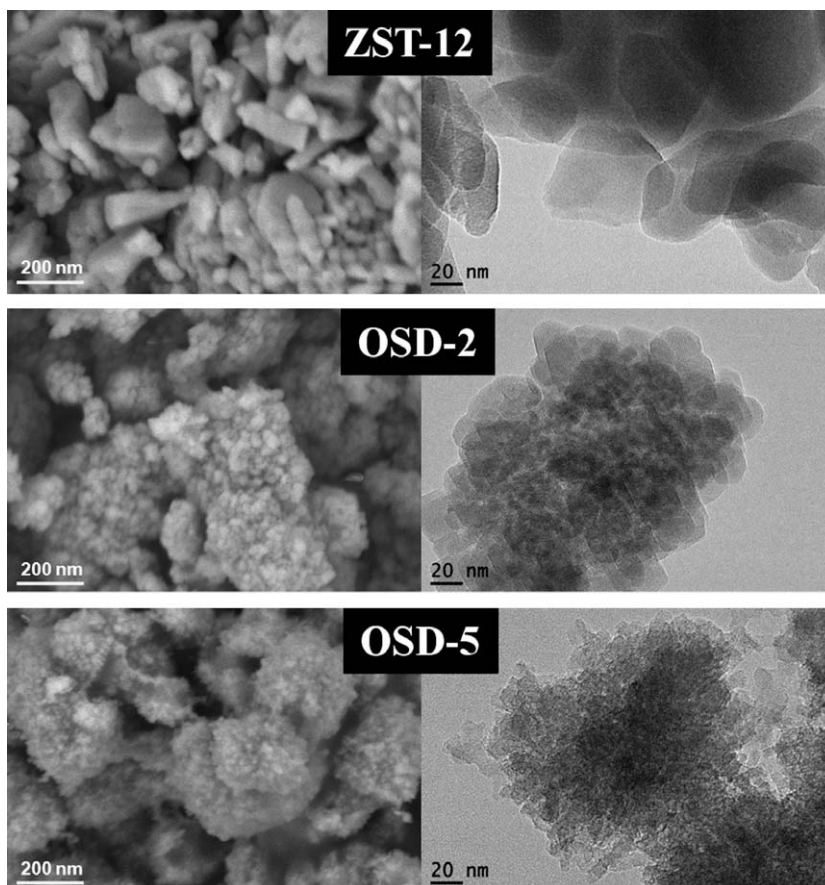

Fig. 2. Electron microscope images (left column: SEM, right column: TEM) of ZST-12, OSD-2, and OSD-5 zeolites.

compared to those of ZST-12 ($388 \, m^2 \, g^{-1}$ and $0.07 \, cm^3 \, g^{-1}$). The pore textural properties are summarized in Table 1. As shown in Fig. 3a, the commercial ZST-12 zeolite showed a typical type-I isotherm corresponding to the mostly microporous structure. On the other hand, OSD-2 and OSD-5 exhibited a type-IV argon adsorption isotherm with an additional capillary condensation step in the mesopores. According to a pore size analysis by the BJH method the mesopore diameters in these samples had a narrow distribution centered on 4 nm. The pore diameters did not noticeably change while the mesopore volume increased according to the TPHAC content in the synthesis composition (Fig. 3b).

The acidity of the zeolite samples was investigated by NH_3 TPD. Fig. 4 shows the NH_3 TPD profiles, which can be deconvoluted to two Gaussian distributions in the region below 800 K. The low-temperature desorption peak (400–600 K) indicates weak adsorption sites, which would catalytically be inactive for MTH reactions [5]. The high temperature peak (600–800 K) was interpreted to be caused by ammonia desorption from strong Brønsted acid sites and strong Lewis acid sites. This peak area allows an estimation of the number of strong acid sites with the assumption of one NH_3 molecule per acid site. The strong acidic sites thus obtained were approximately 25% less in OSD-2 and OSD-5 compared to a commercial ZST-12 sample (Table 2). The acid strengths were very similar. This result is in good agreement with a recent work reported by Suzuki et al., who investigated the acidity of hierarchically porous OSD-type zeolites (the samples were provided by our group) by a combined method of infrared-mass spectroscopy and the TPD of NH_3 [39]. Brønsted acid sites in MFI zeolite are known as MTH catalytic centers [6,40], and the Brønsted sites are normally much greater in number than the Lewis sites. No further quantitative analyses were performed to distinguish strong Brønsted acid sites and strong Lewis acid sites.

3.2. Factors affecting the catalytic lifetime

The catalytic activities for MTH conversion were examined in a fixed bed reactor under identical reaction conditions (reaction temperature: 673 K, WHSV: $7.5 \, g \, g^{-1} \, h^{-1}$) for all MFI zeolites. As shown in Fig. 5a, all the ZST-12, OSD-2, and OSD-5 samples exhibited 100% MTH conversion during the initial reaction period. The product distribution measured at 1 h is presented in Table 3. There
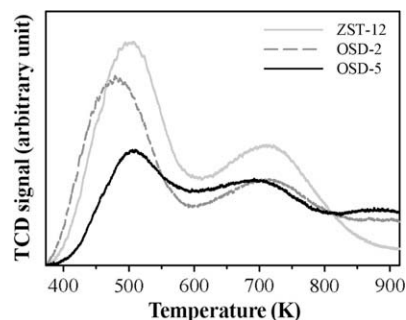

Fig. 4. NH_3 TPD profiles of MFI zeolites. The profiles below 800 K can be deconvoluted to two NH_3 desorption peaks according to Gaussian distributions. The result for OSD-2 and OSD-5 shows an additional peak above 800 K, but it is caused by H_2O generation due to the condensation of silanol groups.

Table 2
Characteristics of acid sites in MFI zeolites and dealuminated OSD-5 samples.

Catalyst	Al content[a] (mmol g^{-1})	Strong acid sites[b] (mmol g^{-1})	External acid sites[c] (mmol g^{-1})
ZST-12	1.30	0.67	0.03
ZST-40	0.41	0.23	–
OSD-2	1.13	0.50	0.13
OSD-5	1.19	0.53	0.23
TA-OSD-5	0.63	0.29	0.05
FS-OSD-5	0.77	0.29	0.14

[a] Estimated by ICP analysis.
[b] From the 600–800 K peak in NH_3 TPD profile.
[c] Calculated by gravimetric measurement of chemisorption of 2,6-di-*tert*-butylpyridine.

was a systematic trend toward increased selectivity for C_2–C_4 olefins and C_{5+} hydrocarbons as the mesoporosity increased. The selectivity for C_6–C_{10} aromatics and C_1–C_4 alkanes decreased (The mesoporosity increased in the order of ZST-12 < OSD-2 < OSD-5 under similar Si/Al ratios). The MTH catalytic activity decreased after an initial reaction period of 10 h. Hereafter the 'catalytic lifetime' was defined as the time at which the catalytic conversion decreased by 50% (i.e., $t_{1/2}$) [41,42]. The $t_{1/2}$ values thus obtained for ZST-12, OSD-2, and OSD-5 were 39, 82, and 132 h, respectively. This result indicates that the catalytic lifetime could show a 3-fold
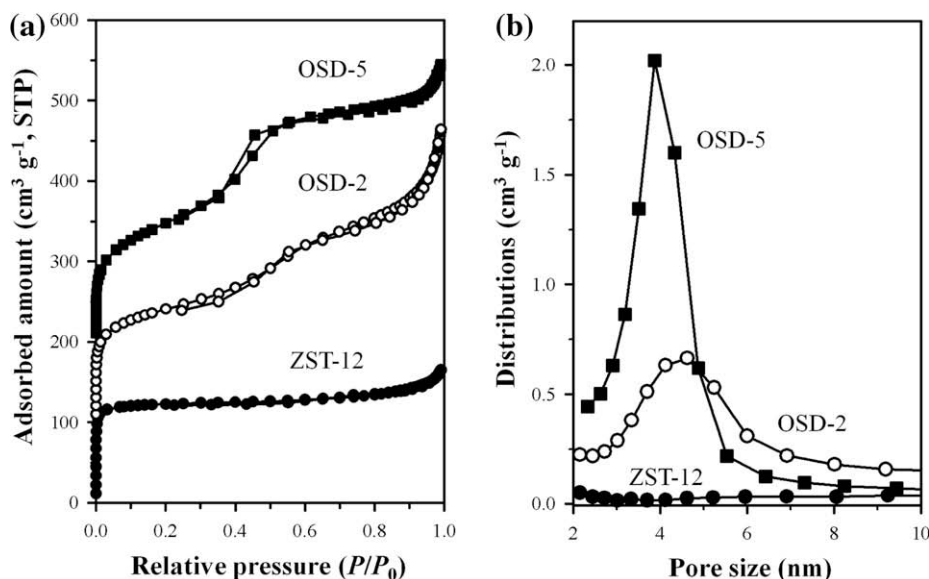

Fig. 3. (a) Argon adsorption–desorption isotherms (87 K) of ZST-12, OSD-2, and OSD-5 zeolites. (b) Corresponding mesopore size distributions analyzed with an adsorption branch using the BJH algorithm. The isotherms for OSD-2 and OSD-5 were offset vertically by 100 and 200 $cm^3 \, g^{-1}$ STP, respectively.
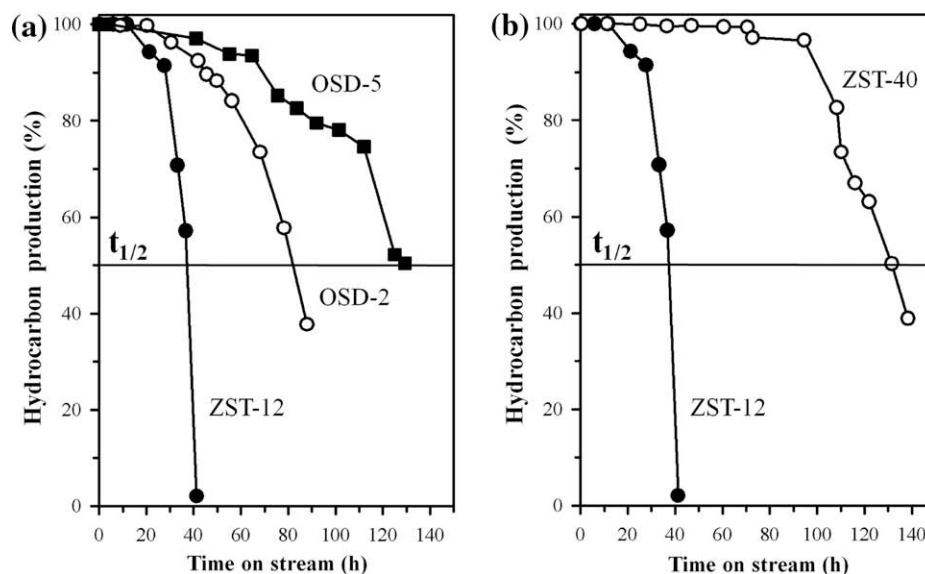
Fig. 5. Catalytic activities for MTH reactions: (a) OSD zeolites with different mesoporosities and (b) ZST zeolites with different Al contents. Hydrocarbon production was calculated by considering methanol and dimethyl ether as unreacted species. '$t_{1/2}$' was used as the catalyst lifetime in the present work.

Table 3
Product selectivity of MTH reactions over MFI zeolites measured at 1 h.

Hydrocarbon selectivity (wt %)	ZST-12	OSD-2	OSD-5
C_1–C_4 alkanes	26.9	22.3	16.9
C_2–C_4 olefins	10.1	13.8	18.3
C_6–C_{10} aromatics	40.1	39.3	33.8
C_{5+}, etc.	22.9	24.6	31.0

Reaction conditions: WHSV of methanol = 7.5 g g^{-1} h^{-1}, catalyst 0.1 g, and temperature 673 K.

improvement due to the generation of mesopores by organosilane surfactants. These $t_{1/2}$ values were compared under very similar Si/Al ratios because the catalytic lifetime is known to change according to the Al content [41–43]. In fact, as shown in Fig. 5b, a bulk MFI sample with Si/Al = 40 (ZST-40) exhibited a much longer lifetime ($t_{1/2}$ = 130 h) than ZST-12 with Si/Al = 12.

The pore textural properties of BTZ-13 and CTZ-16 are given in Table 1. These two samples were obtained via a post-synthetic treatment using NaOH [23] and a hydrothermal synthesis procedure using carbon black as a template [24], respectively. Argon adsorption and TEM investigation proved that both samples possessed intracrystalline mesoporosity, that is, open mesopores within the zeolite crystal (Supplementary material Fig. S1) [23,24]. These zeolites exhibited a significant improvement of the catalyst lifetime ($t_{1/2}$ = 60 h) in MTH reaction, as compared with the result ($t_{1/2}$ = 39 h) of a commercial zeolite sample with a similar Si/Al ratio (Fig. 6a). When $t_{1/2}$ values of various MFI zeolites having similar Al contents were correlated with the external surface areas estimated from a *t*-plot method, there was a good correlation between $t_{1/2}$ and the external surface areas (Fig. 6b). Therefore, it is feasible that the generation of mesopores in MFI zeolite can lead to a significant improvement in the MTH catalytic lifetime, irrespective of the preparation method, when the catalytic lifetime is compared at the same Si/Al ratios.

3.3. Coke location vs. mesoporosity

In order to understand how mesoporosity is related to the catalytic longevity, the commercial ZST-12 and the mesoporous OSD-5 samples were comparatively analyzed using TGA and Ar

adsorption. Particularly, the location and the amount of coke generation were investigated as a function of the reaction time using the characterization method described in Section 2.4. The characterization method is similar to the earlier findings reported by Bibby et al., who studied the location of coke in ZSM-5 using N_2 adsorption [37]. As the result in Fig. 7 shows, there was a remarkable difference between ZST-12 and OSD-5. Coke formed much more rapidly in the solely microporous ZST-12 zeolite than in the highly mesoporous OSD-5 zeolite (50 mg g^{-1} in OSD-5 and approximately 115 mg g^{-1} in ZST-12 at 40 h) during the initial reaction period up to 40 h. Moreover, the coke in ZST-12 was preferentially generated inside micropores prior to the deposition at the external surface. External coke began to form after the micropores were almost completely filled. At *t* = 40 h, hydrocarbon production almost ceased in the case of the solely microporous zeolite. Only dimethylether and unreacted methanol were detected by GC signals. On the other hand, the mesoporous catalyst remained very active up to 120 h. The coke generation was slower, and the coke formed predominantly on the surface of the mesopore walls rather than on the inside of the zeolite micropores.

3.4. Effects of dealumination

In the case of solely microporous MFI zeolites, it was well-known that dealumination could lead to a remarkable increase in the MTH catalytic lifetime [42] prior to the present study. However, little was known about the dealumination effects in the case of mesoporous zeolite. The situation in mesoporous MFI zeolite is complicated by two types of coke deposition sites: the surface of the mesopore walls and the sites inside the micropores. Hence, dealumination was tested in two different ways, as described in Section 2.1.2; the first method used L-tartaric acid and the second involved FS. Tartaric acid has a kinetic molecular diameter of 0.68 nm, which causes a diffusion limitation for dealumination inside micropores (0.56 × 0.53 nm). When the mesoporous OSD-5 zeolite was dealuminated with L-tartaric acid, the Si/Al ratio changed from 13 to 25 (comparing OSD-5 and TA-OSD-5 in Table 1). The number of strong acid sites decreased from 0.53 to 0.29 mmol g^{-1} (Table 2). However, the external acid sites (i.e., acid sites at the mesopore walls) decreased from 0.23 to a very low value of 0.05 mmol g^{-1} (see Section 2.2 for the determination by 2,6-
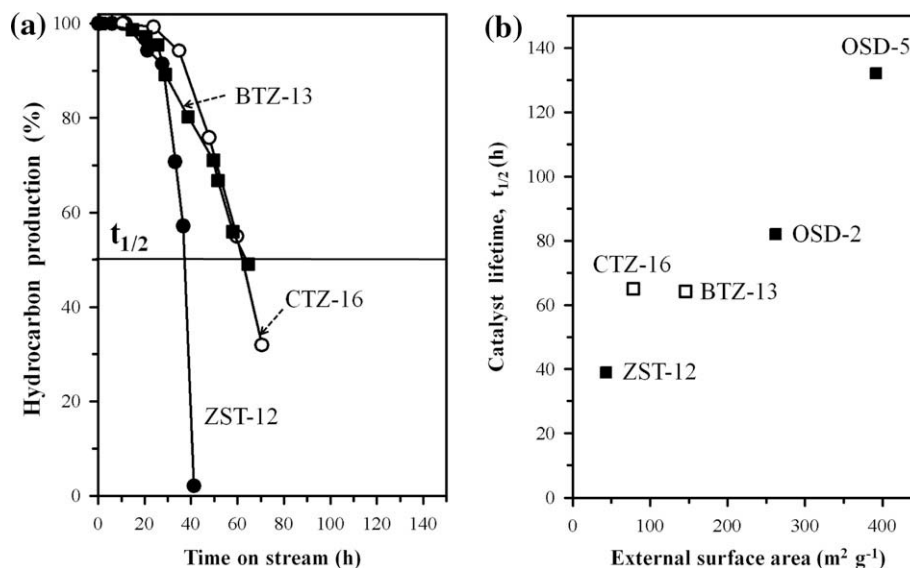
Fig. 6. (a) Catalytic activities of an MTH reaction over two other hierarchical zeolites (BTZ-13 and CTZ-16). (b) Correlation between catalyst lifetime ($t_{1/2}$) and external surface areas.
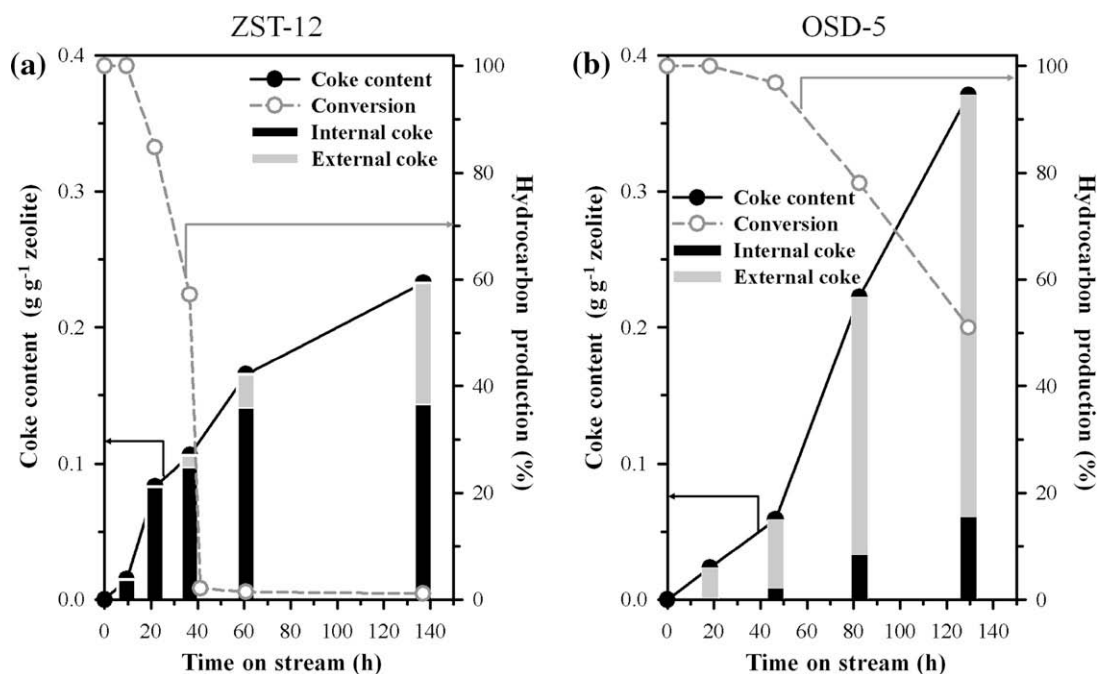

Fig. 7. Coke formation during MTH reactions: (a) solely microporous ZST-12 and (b) highly mesoporous OSD-5 zeolites.

di-*tert*-butylpyridine). Thus, the L-tartaric acid was very effective for selective dealumination from the surface of the mesopore walls [27].

Dealumination with FS attempts a non-selective dealumination process between the surface of the mesopore walls and the area inside the micropores. The experimental conditions were carefully controlled so that the final number of strong acid sites could be as close to the case of TA-OSD-5 as possible. After trial and error, an FS-OSD-5 sample containing the same number of strong acid sites as in TA-OSD-5 was obtained. This sample exhibited 0.14 mmol g^{-1} of external acid sites.

The dealumination effect was investigated with TA-OSD-5 and FS-OSD-5. Both samples exhibited a significant improvement in

their catalyst lifetimes as compared with a pristine zeolite (compared with OSD-5 in Fig. 8a). Between the two dealumination cases, the FS treatment exhibited a very long catalyst lifetime ($t_{1/2}$ = 255 h for FS-OSD-5) as compared with the case of tartaric acid ($t_{1/2}$ = 180 h for TA-OSD-5). That is, dealumination from micropores more effectively improved $t_{1/2}$ compared to treatment at the surface of the mesopore walls. Another notable point is that both OSD-5 and TA-OSD-5 showed very similar coke locations when their reaction times were normalized to the same time scale of $t/t_{1/2}$ (comparing Figs. 7b and 8b). Despite the almost complete removal of external acid sites, coke in TA-OSD-5 was nonetheless generated at the external surfaces. The catalytic lifetime of TA-OSD-5 was shorter than that of FS-OSD-5.
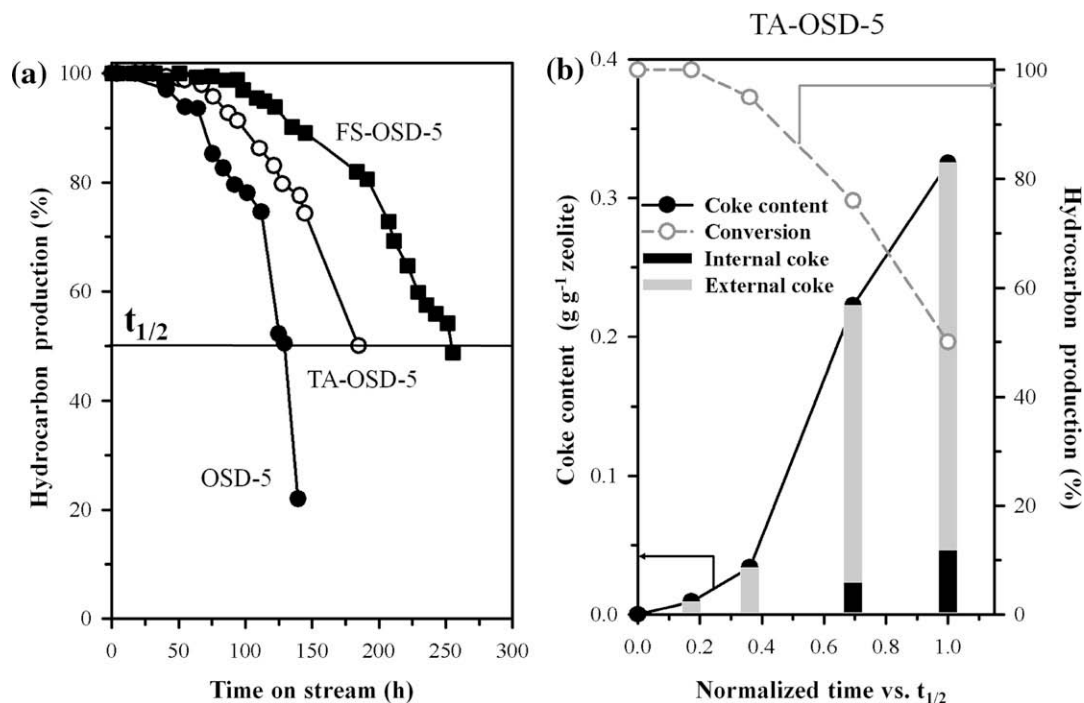
Fig. 8. (a) Catalytic activities for an MTH reaction over OSD-5 and its dealuminated samples treated with L-tartaric acid (TA-OSD-5) and fluorosilicate (FS-OSD-5), respectively. (b) Coke formation in TA-OSD-5 during the reaction. The time scale was normalized by the $t_{1/2}$ value of TA-OSD-5.

4. Discussion

MTH reactions can be catalyzed by the strongly acidic zeolites HZSM-5 and Hβ [5]. Acidic zeolite analogues SAPO-34 and SAPO-18 are also effective catalysts [5]. Early investigations proposed that the reactions would be directly catalyzed by a strong acid site in a zeolite cage. More recent investigations revealed that the reactions, at least MTO, should be catalyzed through what is known as the hydrocarbon pool mechanism in which a methylated aromatic hydrocarbon inside a zeolite pore would be an active center for product generation [7,12–14]. The primary products are ethylene and propylene, and these molecules can undergo further reactions that lead to the formation of higher hydrocarbons, such as polymerization, isomerization, aromatization, cracking, and hydrogenation. The zeolite catalyst becomes progressively deactivated as some of these bulky hydrocarbons remain inside the zeolite cages and thereby block the access of reactant molecules [12,44].

HZSM-5 zeolite is often chosen as an MTG catalyst owing to its high product selectivity in the gasoline-range, high catalytic activity, and long catalytic lifetime among zeolites. A high Si/Al ratio is preferred because zeolite with a low concentration of acid sites is deactivated more slowly. In addition to the effect of the Si/Al ratio, the deactivation rate is known to be dependent on the reactant composition, reaction temperature, pore diameter of the catalyst, and strength of the acid sites [6]. Early studies of MTG over the HZSM-5 zeolite reported that the catalysts were deactivated progressively as the micropores became filled with coke species before the coke was generated at the external surface [6,37,38,45]. In contrast, later works showed that HZSM-5 catalysts were deactivated slowly as graphitic coke was generated on the external surface before the formation of internal coke [13,46]. This discrepancy can be understood in terms of the differences in the Si/Al ratio. The coke formation and deactivation behavior of ZST-12 (conventional HZSM-5, Si/Al = 12) presented in Fig. 7 is similar to the results reported in early studies. On the other hand, the ZST-40 (conventional HZSM-5, Si/Al = 40) catalyst sample here exhibited the

generation of external coke prior to micropore filling (as reported in Fig. 4 of Ref. [47]). The zeolite sample continued to exhibit catalytic activity as long as internal micropores were accessible. The rate of the internal coke formation decreased as the concentration of strong acid sites in the HZSM-5 zeolite decreased thereby increasing the catalytic lifetime.

Recently, catalytic lifetimes that were 1.5–2 times the normal lifetime were reported with hierarchically porous MFI zeolites as compared with solely microporous zeolites [32,33]. However, no quantitative correlations between mesoporosity and the catalytic lifetime were reported in the previous studies. In the present work, three methods were independently used to prepare catalyst samples with a wide variation in their mesoporosity, for example, a synthesis method using an organosilane surfactant, a method involving the use of a carbon template, and a method involving a post-synthetic alkali treatment. Catalytic lifetimes were measured within a series of MFI samples with a wide variation of mesoporosity, while the variation of the Si/Al ratios was maintained in a narrow range. This allowed the effect of different Al contents (or the content of strong acid sites) to be isolated, giving a generalized and quantitative correlation between mesoporosity and catalytic lifetime as shown in Fig. 6b. The resulting correlation in Fig. 6b shows that the catalytic activity increased to three times in an approximately linear manner when plotted with respect to the external surface area (i.e., mesopore walls).

In recent years, catalytic longevity of hierarchically porous zeolites was also confirmed in other acid-catalyzed reactions. The results were attributed to enhanced molecular diffusions through the mesopores [31]. Hierarchical zeolites exhibited a 100-fold increase in their diffusion rate as compared to solely microporous zeolites [48]. In the previous studies, however, there were no explanations of how fast diffusion can lead to catalytic longevity. Here, the effect of mesoporosity against the deactivation has been more clearly established by probing the location of coke formation during the MTH reaction. In the presence of mesoporosity, coke was deposited on the external surfaces more than it was inside the micropores

(see Fig. 7). This result can be attributed to the enhanced mass transfer of coke precursors (e.g., olefinic and aromatic species). Due to the enlarged external surface area and short diffusion path lengths, it is feasible that the coke precursors that formed inside the micropores readily migrated to the external surface. In the case of solely microporous zeolites, the diffusion of the coke precursors from the micropores to the external surface would be relatively slow. The coke precursors could react further to polymerize within the micropores to form internal coke. This type of internal coke can play a more deteriorative role in the deactivation due to the direct coverage on strong acid sites and also indirectly by blocking diffusion into other micropores [6]. In contrast, the external coke was less effective in blocking access to the active sites unless the pore entrances were completely covered [6,37]. The loss of catalytic activity by the two coke locations (i.e., internal coke and external coke) is well represented in Fig. 7. The catalytic activity of ZST-12 was significantly affected, even at low coking levels, due to the formation of internal coke. However, the catalytic activity of the mesoporous OSD-5 catalyst remained high even after external coke became heavily deposited. Thus, the mesoporous catalysts exhibited high resistance to catalyst deactivation.

Combining the mesopore effect and the Si/Al effect, it is reasonable that the catalytic lifetime would increase much more if a zeolite sample with a low number of strong acid sites and high mesoporosity was used as a catalyst. In fact, such an MFI zeolite was very recently synthesized in our laboratory using an organic surfactant containing a di-quaternary ammonium head group [47]. The MFI zeolite synthesis was performed via an MFI structure-directing action in the surfactant head group without an additional MFI structure-direction agent such as tetrapropylammonium ions. The MFI zeolite was composed of extremely thin nanosheets (Si/Al = 50) corresponding to a single unit-cell dimension along the b-axis. The BET surface area of this zeolite was 700 m^2 g^{-1}. This zeolite exhibited a tremendously enhanced catalyst lifetime ($t_{1/2} \approx 26$ days; five times longer than ZST-40) under an MTH reaction condition. This is similar to the present experimental condition (at 673 K, WHSV = 11 g g^{-1} h^{-1}) [47].

In addition to the effect of mesoporosity, the role of external acid sites in the deactivation is another interesting factor to consider in the design of a catalyst with a superior lifetime. It is often speculated that the external acid sites should strongly influence external coke formation and hence the catalyst lifetime in MTH reactions [6]. Suzuki et al. reported that lowering the external Al content could suppress coke deposition and improve catalyst stability [49,50], although their study was limited to conventional zeolites having a low external surface area. In comparison, the present dealumination experiment (Section 3.4) involving hierarchical zeolites revealed that the internal acid sites were mainly responsible for improving the catalyst lifetime. Furthermore, although external acid sites were almost completely removed, coke formation and the associated locations were nonetheless similar to the result obtained before dealumination. This result suggests that coke generation (the rate and location) can be determined according to the mesoporosity (or wall thickness), though it can be mainly determined according to the number and strength of the acid sites that are located inside the micropores rather than those located on the external surface.

MFI catalysts can be regenerated by removing the coke through calcination in air at high temperatures (>773 K). According to the previous works, a repeated regeneration process via a calcination treatment led to a gradual decrease in the framework Al quantity resulting in a progressive increase in the catalyst lifetime rather than the deterioration of the catalytic performance [42]. The dealumination is caused by the steam that is produced during the oxidation of coke at high temperatures. Our mesoporous OSD-5 zeolite also exhibited a similar regeneration behavior.

5. Conclusions

This study outlines the 5-fold increase in the catalytic lifetime of an MFI zeolite in a MTH reaction that is caused by the mesoporosity. A roughly linear correlation between the mesoporosity and the catalytic lifetime was confirmed. The origin of catalytic longevity can be explained in terms of the facile diffusion of coke precursors from the micropores to the external surfaces (or the surfaces of the mesopore walls) owing to a large external surface area and short diffusion path lengths. Catalytic deactivation under the present reaction conditions occurred almost as a result of the formation of internal coke, that is, as a result of coke inside micropores. Selective dealumination at the surface of the mesopore walls caused no significant change in the coke generation ratio between internal and external locations. Removal of internal Al led to a marked increase in the catalyst lifetime.

Catalytic activity did not change sensitively to the generation of mesoporosity. Hence, for an MFI zeolite with a high catalytic activity and a long lifetime, the mesoporosity should be maximized (or the wall thickness should be minimized). The framework Si/Al ratio may be optimized separately. Mesoporous zeolites thus optimized would improve the MTG process efficiency and bring down the overall costs for industrial production. It would be interesting if the present conclusions could be generalized to a variety of other acid-catalyzed reactions and for other hierarchically porous zeolites with different pore topologies. Further studies are in progress in our laboratory.

Acknowledgments

Appendix A. Supplementary material

Supplementary data associated with this article can be found, in the online version, at doi:10.1016/j.jcat.2009.11.009.

References

[1] J.H. Lunsford, Catal. Today 63 (2000) 165.
[2] M. Stöcker, Angew. Chem. Int. Ed. 47 (2008) 9200.
[3] A.H. Khodakov, W. Chu, P. Fongarland, Chem. Rev. 107 (2007) 1692.
[4] P.J. van Berge, in: S.H. Moon (Eds.), Abstracts of Papers, 14th International Congress on Catalysis, Seoul, Korea, July 2008, Abstract PL04.
[5] M. Stöcker, Microporous and Mesoporous Mater. 29 (1999) 3.
[6] D.M. Bibby, R.F. Howe, G.D. McLellan, Appl. Catal. A: Gen. 93 (1992) 1.
[7] J.F. Haw, W. Song, D.M. Marcus, J.B. Nicholas, Acc. Chem. Res. 36 (2003) 317.
[8] F.J. Kiel, Microporous and Mesoporous Mater. 29 (1999) 49.
[9] C.S. Cundy, P.A. Cox, Chem. Rev. 103 (2005) 663.
[10] C.D. Chang, A.J. Silvestri, J. Catal. 47 (1977) 249.
[11] C.D. Chang, Catal. Rev. 25 (1983) 1.
[12] U. Olsbye, M. Bjørgen, S. Svelle, K.P. Lillerud, S. Kolboe, Catal. Today 106 (2005) 108.
[13] M. Bjørgen, S. Svelle, F. Joensen, J. Nerlov, S. Kolboe, F. Bonino, L. Palumbo, S. Bordiga, U. Olsbye, J. Catal. 249 (2007) 195.
[14] D.M. McCann, D. Lesthaeghe, P.W. Kletnieks, D.R. Guenther, M.J. Hayman, V.V. Speybroeck, M. Waroquier, J.F. Haw, Angew. Chem. Int. Ed. 47 (2008) 5179.
[15] W.J.H. Dehertog, G.F. Froment, Appl. Catal. 71 (1991) 153.
[16] C.J. Maiden, Stud. Surf. Sci. Catal. 36 (1988) 1.
[17] J.Q. Chen, A. Bozzano, B. Glover, T. Fuglerud, S. Kvisle, Catal. Today 106 (2005) 103.
[18] J.R. Rostrup-Nielsen, Catal. Today 37 (1997) 225.
[19] A.T. Aguayo, A.G. Gayubo, J.M. Ortega, M. Olazar, J. Bilbao, Catal. Today 37 (1997) 239.
[20] Y. Tao, H. Kanoh, L. Abrams, K. Kaneko, Chem. Rev. 106 (2006) 896.
[21] K. Egeblad, C.H. Christensen, M. Kustova, C.H. Christensen, Chem. Mater. 20 (2008) 946.
[22] J. Pérez-Ramírez, C.H. Christensen, K. Egeblad, C.H. Christensen, J.C. Groen, Chem. Soc. Rev. 37 (2008) 2530.
[23] J.C. Groen, J.C. Jansen, J.A. Moulijn, J. Pérez-Ramírez, J. Phys. Chem. B 108 (2004) 13062.

[24] C.J.H. Jacobsen, C. Madsen, J. Houzvicka, I. Schmidt, A. Carlsson, J. Am. Chem. Soc. 122 (2000) 7116.

[25] H. Wang, T.J. Pinnavaia, Angew. Chem. Int. Ed. 45 (2006) 7603.

[26] M. Choi, H.S. Cho, R. Srivastava, C. Venkatesan, D.H. Choi, R. Ryoo, Nature Mater. 5 (2006) 718.

[27] V.N. Shetti, J. Kim, R. Srivastava, M. Choi, R. Ryoo, J. Catal. 254 (2008) 296.

[28] Y. Sun, R. Prins, Appl. Catal. A: Gen. 336 (2008) 11.

[29] C.H. Christensen, K. Johannsen, I. Schmidt, C.H. Christensen, J. Am. Chem. Soc. 125 (2003) 13370.

[30] J.S. Jung, J.W. Park, G. Seo, Appl. Catal. A: Gen. 288 (2005) 149.

[31] R. Srivatava, M. Choi, R. Ryoo, Chem. Commun. (2006) 4489.

[32] T.V.W. Janssens, S. Dahl, C.H. Christensen, US Patent (2006) 7 078 578.

[33] M. Bjørgen, F. Joensen, M.S. Holm, U. Olsbye, K.-P. Lillerud, S. Svelle, Appl. Catal. A: Gen. 345 (2008) 43.

[34] S. Kumar, A.K. Sinha, S.G. Hedge, S. Sivasanker, J. Mol. Catal. A: Chem. 154 (2000) 115.

[35] S. Lowell, J.E. Shields, M.A. Thomas, M. Thommes, in: B. Scarlett (Ed.), Characterization of Porous Solids and Powders: Surface Area, Pore Size and Density, Kluwer Academic, Dordrecht, 2004, p. 147.

[36] D.R. Dubois, D.L. Obrzut, J. Liu, J. Thundimadathil, P.M. Adekkanattu, J.A. Guin, A. Punnoose, M.S. Seehra, Fuel Process. Technol. 83 (2003) 203.

[37] D.M. Bibby, N.B. Milestone, J.E. Patterson, L.P. Aldridge, J. Catal. 97 (1986) 493.

[38] D.M. Bibby, C.G. Pope, J. Catal. 116 (1989) 407.

[39] K. Suzuki, Y. Aoyagi, N. Katada, M. Choi, R. Ryoo, M. Niwa, Catal. Today 132 (2008) 38.

[40] H. Itoh, C.V. Hidalgo, T. Hattori, M. Niwa, Y. Murakami, J. Catal. 85 (1984) 521.

[41] K.G. Ione, G.V. Echevskii, G.N. Nosyreva, J. Catal. 85 (1984) 287.

[42] S.M. Campbell, D.M. Bibby, J.M. Coddington, R.F. Howe, J. Catal. 161 (1996) 350.

[43] D.B. Luk'yanov, Zeolites 12 (1992) 287.

[44] D.M. Marcus, W. Song, L.L. Ng, J.F. Haw, Langmuir 18 (2002) 8386.

[45] A.D. Lucas, P. Canizares, A. Durán, A. Carrero, Appl. Catal. A: Gen. 156 (1997) 299.

[46] L. Palumbo, F. Bonino, P. Beato, M. Bjørgen, A. Zecchina, S. Bordiga, J. Phys. Chem. C 112 (2008) 9710.

[47] M. Choi, K.-S. Na, J. Kim, Y. Sakamoto, O. Terasaki, R. Ryoo, Nature 461 (2009) 246.

[48] J.C. Groen, W. Zhu, S. Brouwer, S.J. Huynink, F. Kaptejin, J.A. Moulijn, J. Prez-Ramez, J. Am. Chem. Soc. 129 (2007) 355.

[49] K. Suzuki, Y. Kiyozumi, K. Matsuzaki, S. Shin, Appl. Catal. 35 (1987) 401.

[50] K. Suzuki, Y. Kiyozumi, K. Matsuzaki, S. Shin, Appl. Catal. 42 (1988) 35.